



C-V AND I-V CHARACTERISTICS OF In_2O_3 / GaAs HETEROJUNCTION

Iftikhar M.Ali , Issam M.Ibrahim, Iqbal S.Naji

University of Baghdad, College of Science, Physics Depart., Al-Jadiriya, Iraq
iftikhariq@gmail.com,

Received 20-01-2013, online 30-01-2013

ABSTRACT

Polycrystalline In_2O_3 Thin films have been prepared by flash evaporation. The crystal structure of as deposited and annealed at 523K was investigated by using X-ray diffraction. The Hall Effect measurements confirmed that electrons were predominant charges in the conduction process (i.e n-type). It is found that the absorption coefficient of the prepared films decreases with increasing T_a . The d.c. conductivity study showed that the conductivity increase with increasing T_a , whereas the activation energy decreases with increasing T_a . The barrier tunneling diode for In_2O_3 /n-GaAs (100 orientation) heterostructure grown by Flash evaporation technique was studied. (capacitance-voltage C-V) spectroscopy measurements were performed at 303 K and at the annealing temperature 523K. The built in voltage has been determined and it depends strongly on the annealing process of the heterojunction. From I-V characteristics the ideality factor was calculate, and found that it decreases when increasing annealing temperature.

Keywords: Flash evaporation, GaAs heterojunction, In_2O_3 film.

I. INTRODUCTION

III-V semiconductors and GaAs in particular, seem to be useful as optoelectronic devices working in the visible wavelength region [1,2]. However, little interest is being shown towards amorphous III-V semiconductors. This is presumably due to the fact that the physics of these materials is not yet completely understood. The study of the obtained heterojunctions can be useful in obtaining an insight into amorphous crystalline (a/c) junction properties in order to improve heterojunction devices. Important new applications are possible today in the field of energy conversion and storage by the application of thin and nanostructure solid films on surfaces. These special films, or multiple films, will be integral parts of the energy systems in the near future for the production of useful thermal and electrical energy and for energy saving application [3]. Among the metal-oxide structures, a unique and particularly interesting material is indium oxide (In_2O_3). In_2O_3 has also attracted considerable research. It is known to have a body centered cubic structure ($a = 10.12 \text{ \AA}$)[4]. In_2O_3 has been widely used in the microelectronic field as gas detectors, window heaters, solar cells, memory devices, and flat panel display materials [4–13]. Indium oxide is one of the most promising polycrystalline materials for thin film solar cells due to its physical properties: It has high

absorption coefficient (larger than 10^5 cm^{-1} at wavelength 600nm) so that only thin layers (a few microns) are needed for the absorption of the most solar spectra photons with energy higher than band gap [14]. Indium (III) oxide (In_2O_3) is an amphoteric oxide of indium. It is an n-type semiconductor and it forms bixbyite type cubic crystals. Its band gap has recently been to 2.9 eV [15]. Indium oxide is used in some types of batteries, thin film infrared reflectors transparent for visible light (hot mirrors), optical coatings, antistatic coatings, photocatalyst sensors, etc. It is also used in resistive elements and integrated circuits. When it is combined with tin oxide, it forms indium tin oxide, traditionally known as ITO, and used for transparent conductive coatings. In histology, indium oxide is used as a part of some stain formulations. Thin films of chromium-doped indium oxide ($\text{In}_{2-x}\text{Cr}_x\text{O}_3$) were recently reported to be magnetic semiconductors displaying high-temperature ferromagnetism, single-phase crystal structure, and semiconductor behavior with a high concentration of charge carriers. It has possible applications in spintronics as a material for spin injectors [15,16]. GaAs-BASED heterojunction have long been recognized as the leading device technology for high-speed high-power applications. With the increased

popularity of wireless communications, extending the HBTs' capability into even higher power for base-station applications is quite obvious [17].

II. EXPERIMENTAL PROCEDURE

Thin In₂O₃ films were deposited on corning glass substrate and GaAs (n-type (100) orientation), using flash evaporation method under vacuum environment 10⁻⁵ mbar. The evaporation powder was continuously dropped into the molybdenum boat heated at a temperature of about 1600K by using vacuum unit model Edward (216E). The film thickness was (100±15 nm). Annealing treatment of thin In₂O₃ films was carried out in air for duration 1 hour at temperature of 523K .the structure of the films was examined via X-ray diffraction (XRD-6000-shemadzu with CuK_α, wave length of 1.54Å⁰). Al metal contact electrodes were thermally

III. RESULTS AND DISCUSSION

The X-ray diffraction of In₂O₃ films at 303K and 523K were carried out in order to get an information about the crystal structure and any changes produced in this structure by heat treatment for these films .Obviously, the structure of the as deposited In₂O₃ films and annealed at 523K are polycrystalline structure as shown in Fig.(1),However, the intensity of annealed sample increases with increase annealing temperature this is may be due to the increasing in grain size or the arrangement in the structure. It can be inferred from Table 1 comparable values of diffracted angle (2θ), inter-planner distance(d) of the peaks of deposited and annealing samples.

Table 1: The value of (2θ) and inter-planner distance (d) of Indium oxide thin films at 303K and annealed at 523K

Experimental		Standard (ASTM)		
2θ (deg)	d (Å)	2θ (deg.)	d (Å)	hkl
17.1	5.179	17.512	5.09	200
20.71	4.283	21.49	4.13	211
35.50	2.525	35.466	2.527	400

The electrical properties of the films were found to be related to the microstructure and crystallographic structure which is in turn strongly depend on the annealing temperature.

deposited in vacuum 10⁻⁵ mbar, coated electrode was 300nm thick. The glass substrates were cleaned by degenerate solution and rinsed with water and afterward they ultrasonically cleaned in acetone bath for 10 min. finally they were rinsed with distilled water. The substrate temperature during the deposition process was kept at 303K.

The UV-Visible optical transmission spectra of the thin films were recorded (Shemadzu UV-160/UV-Visible spectrophotometer) and the films investigated by means of experimental measurements of transmittance were in the range (400-900 nm). Dc electrical conductivity, Hall effect were measured to determine the electrical transport properties and the type of Indium Oxide film (a digital electrometer type Keithley 616 was used for these purpose). The C-V characteristic were carried out using LCR meter model [HP-R2CC4274].

The variation of $Ln\sigma$ as a function of reciprocal temperature for as deposited and annealed films at 523K is shown in Fig.(2) The plots suggest that there are two distinct regions corresponding to low and high temperatures (303-473K) for deposited and annealed at 523K. The d.c conductivity exhibits an activated temperature dependence, in accordance with the stuckes equation [18]

$$\sigma = \sigma_0 Exp.(-E_c - E_f/k_B T) \quad (1)$$

where σ_0 is minimum metallic conductivity ($E_c - E_f$) is the activation energy for electrons conduction, k_B is the Boltzmann constant and T is the temperature (K). At higher temperature ranges the conduction mechanism of this stage is due to carriers excited into extended states beyond the mobility edge and for the other temperature range the conduction mechanism is due to carriers excited into localized states at the edge of band edges and hopping at energy close to the tail, while for annealing samples there one mechanism of conductivity, so the mechanism of this stage is due to carriers excited into extended states (see Table 2).

The transparency of thin films for deposited and annealing samples exhibits a sharp decrease in the UV region as shown in Fig.(3).

The transmission percent of In₂O₃ films were also changed from 80% to 60% in the 900nm region for deposited and annealed at 523K, respectively. All the samples show optical transparency in the spectral region (500-900nm). The transmittance decreases in the band gap region for annealing

treatment films. The absorption coefficient (α) can be calculated from the relation [19]

$$\alpha = 2.303 A_0/t \quad (2)$$

where A_0 is absorption t is thickness of the film. The optical band gap values of the In_2O_3 films were obtained by plotting $(\alpha h\nu)^2$ against $(h\nu)$ as shown in Fig.(4). The linear nature of the plot after the absorption edge indicates the presence of direct transition. The extrapolated of the linear portion to the x-axis gives the values of optical band gap (E_g) which are 2 eV and 1.65 eV for as deposited and annealed at 523K for 1hr respectively. The value of energy gap is less than that obtained by Luis et.al [20], because of the difference of preparation conditions. The data of Fig.(4) clearly shows the progressive sharpening of the absorption edge upon heat treatment, the reason for the sharpening might be due to a change in the stoichiometry or intrinsic (defect population of the heat treatment samples [21-23].

The variation of capacitance as a function of forward and reverse bias voltage in the range of (0-0.5) Volt at frequency equal to 400 kHz has been studied, for $\text{In}_2\text{O}_3/\text{n-GaAs}$ heterojunction for deposited and for annealing samples. The inverse capacitance square is plotted against applied voltage as shown in Fig.(5). The plots revealed straight line relationship which means that the

junction was of an abrupt type. This is in agreement with the result of Ryu and Takashi [24], Jain and Melehy [25]. The interception of the straight line with the voltage axis at $(1/C^2)=0$ represents the built-in voltage [26]. We observed from Table (2) that the built-in voltage decreases with increasing of T_a as a result of the increases in the capacitance value and the decrease of the depletion width.

The properties of the interface vary greatly from material to material and largely depend on the method of formation. The main parameters of energy band diagram are ΔE_v and ΔE_c which can be calculated from equation (3 to 5) [27] :

$$\Delta E_c = \chi_n - \chi_p \quad (3)$$

$$\Delta E_v = (E_{gp} - E_{gn}) - (\chi_n - \chi_p) \quad (4)$$

$$\Delta E_v = V_{bi} + E_{an} + E_{ap} - E_{g1} \quad (5)$$

where V_{bi} is the Built-in potential, E_{an}, E_{ap} the activation energy for n and p-type semiconductor, E_{g1}, E_{g2} the optical energy gap for n and p-type semiconductors. Experimentally it is found that the two semiconductors have different energy gaps (E_g), different dielectric constants (ϵ), different work functions (ϕ) and different electron affinity values (χ).

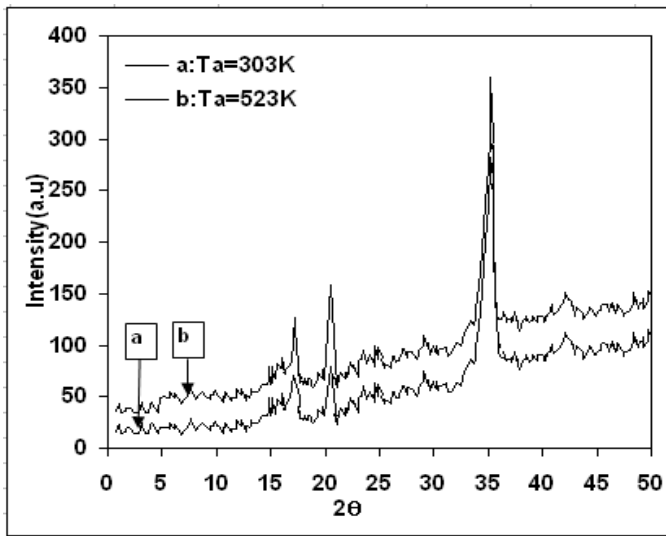


Fig. (1): XRD spectrum of the-deposited In_2O_3 thin films, and for annealed at 523K.

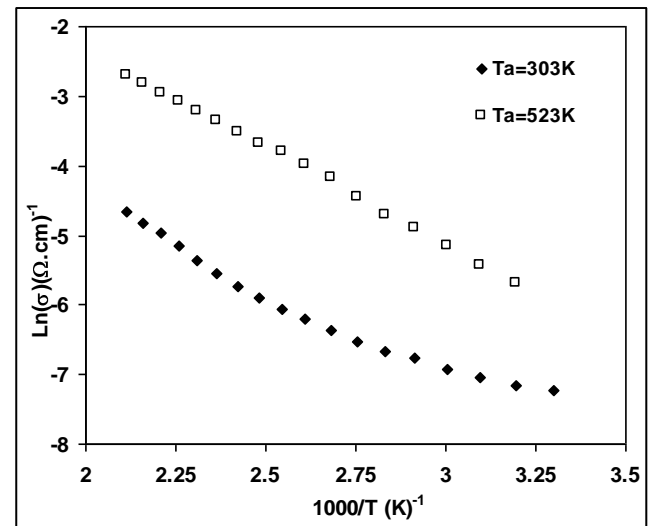


Fig. (2): Temperature dependence of D.C. conductivity σ of the-deposited In_2O_3 thin films, and for annealed at 523K

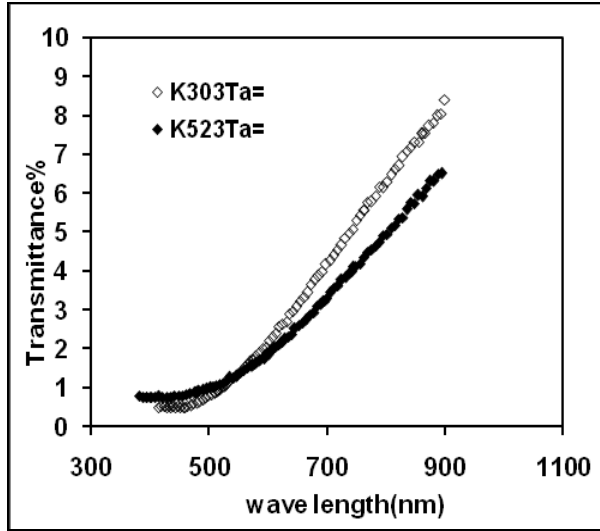


Fig. (3): Transmittance spectrum for-deposited In_2O_3 thin films, and for annealed at 523K

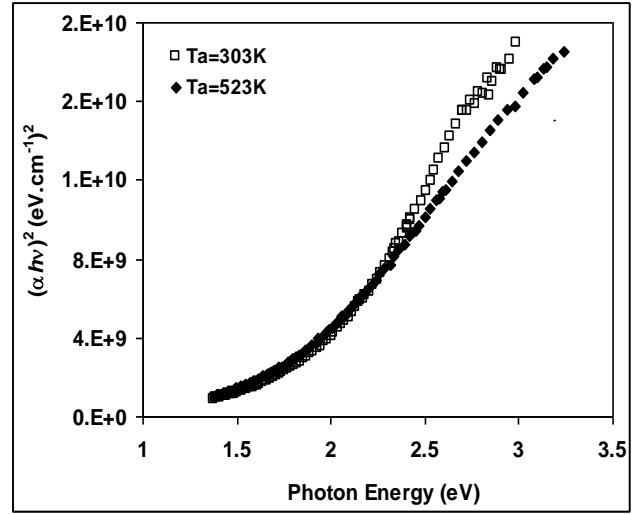


Fig. (4): $(\alpha h\nu)^2$ vs. $h\nu$ for samples prepared and for annealed at 523K

Table (2): The activation energy, optical energy gap, difference in valence and conduction band, and ideality factor.

In_2O_3 films				$\text{In}_2\text{O}_3/\text{n-GaAs}$ HJ			
T_a (K)	E_{a1} (eV)	E_{a2} (eV)	E_g (eV)	ΔE_v (eV)	ΔE_c (eV)	V_{bi} (eV)	β
303	0.11	0.26	2.0	0.12	0.46	1.34	1.373
523	-----	0.25	1.65	0.04	0.19	1.04	1.087

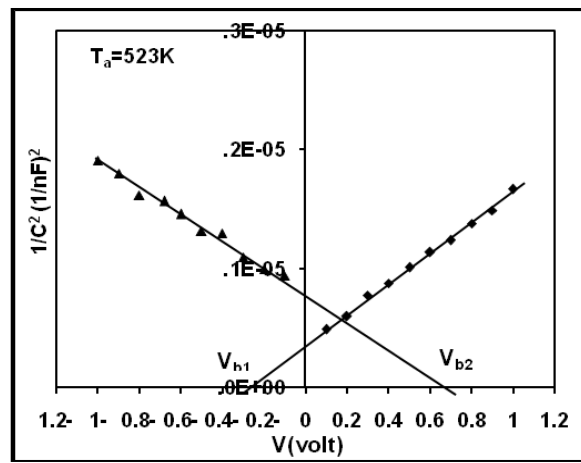
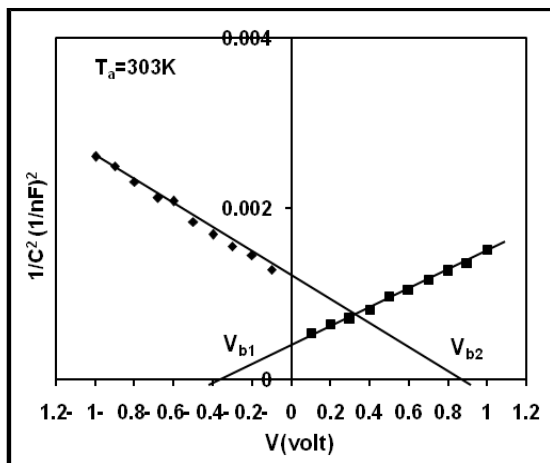


Fig. (5): Built-in voltage of the as-deposited $\text{In}_2\text{O}_3/\text{n-GaAs}$ heterojunction, and annealed at 523K

The current–voltage characteristic parameters are important to identify the significance of the various components under reverse and under forward bias. We can find some important parameters.

Fig.(6) shows the I-V characteristic for In₂O₃/n-GaAs HJ at forward bias voltage within the range (0-0.5 Volt) for forward bias voltage.

The applied voltage injects majority carriers which decreases the built-in potential, as well as the width of the depletion layer. The majority carrier concentration is higher than the intrinsic carrier concentration which generates the recombination current in the low voltage region (0-0.3 Volt). This is because the excited electrons from valance band

to conduction band will recombine them with holes that are found at the (V.B). This is observed by the little increase in the recombination current at low voltage region [28].

The ideality factor gives indication about the defects in the junction, which could be calculated from [29]

$$\beta = \frac{q}{k_B T} \frac{V}{\ln(I_f/I_s)} \dots\dots\dots(6)$$

a high value indicates structural defects [30]. These values are in agreement with those found by Milnes and Feucht [31] [see table 2.

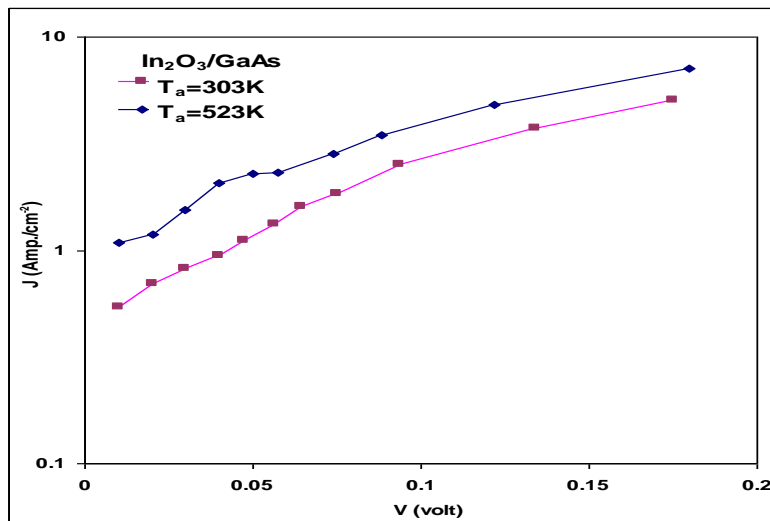


Fig.(6): I-V characteristics at forward bias voltage for In₂O₃/n-GaAs HJ

IV. CONCLUSION

In₂O₃ films are prepared successfully by thermal evaporation technique, the structure of deposited In₂O₃ film and that which annealed at 537K are polycrystalline. The conduction mechanism of films reveals that at higher temperature ranges the conduction mechanism is extended states beyond the mobility edge, and for low temperature ranges the conduction mechanism is due to carriers excited into localized states at the edge of band and hopping at energy close to the tail. The optical energy gap E_g decreases with increasing annealing temperature from 2.0 to 1.65eV which made this material is suitable for solar cell devices. The junction was of abrupt type. The ideality factor reveals high values, this is because of the structural defects.

References

- [1] N.I.Aly, A.A.Akl, A.A.Ibrahim, and A.S.Riad, " Carrier Transport Mechanisms of a-GaAs/ n-Si Heterojunctions", Phys.Stat. Sol. (a), 24, 245-254 (2001).
- [2] J.Bandet, Kh.Aguir, D.Lollman, A.Fennouh& H.Carchano, "Raman and Electrical Characterizations of a-GaAs_{1-x}N_x Thin Films Grown on c-Si(p) Substrates by N₂ Reactive Sputtering", Jpn. J.Appl. Phys.36, 11-18 (1997).
- [3] Yianoulis P. and Giannouli M., "Thin Solid Films Conversion and Energy Saving Applications", J. Nano Search 2 ,49-60 (2008).
- [4] L. Dai, X. L. Chen, J. K. Jian, M. He, T. Zhou and B. Q. Hu, "Fabrication and Characterization of In₂O₃Nanowires", Appl. Phys. A Mater. Sci. Process., 75, 687–689 (2002).

- [5] J. R. Bellingham, A. P. Mackenzie, and W. A. Philips, "Precise Measurements of Oxygen Content: Oxygen Vacancies in Transparent Conducting Indium Oxide Films", *Appl. Phys. Lett.*, **58**, 2506–2508 (1991).
- [6] K. Osaza, T. Ye, and Y. Aoyagi, "Deposition of Thin Indium Oxide Film and Its Application to Selective Epitaxy for In Situ Processing", *Thin Solid Films*, **146**, 58–64 (1994).
- [7] I. Hamberg and C. G. Granquist, "Evaporated Sn-Doped In₂O₃ Films: Basic Optical Properties and Applications to Energy-Efficient Windows", *J. Appl. Phys.*, **60**, 123–160 (1996).
- [8] M. Jung, H. Lee, S. Moon, W. Song, N. Kim, J. Kim, G. Jo, and T. Lee, "Short-Channel Effect and Single-Electron Transport in Individual Indium Oxide Nanowires", *Nanotechnology*, **18**, 435-403 (2007).
- [9] M. H. Habibi, T. Nasrin, and C. J. Ha, "Characterization and Photocatalytic Activity of Nanostructured Indium Tin Oxide Thin-Film Electrode for Azo-Dye Degradation", *Thin Solid Films*, **515**, 1461–1469 (2006).
- [10] P. Xu, Z. Cheng, Q. Pan, J. Xu, Q. Xiang, W. Yu, and Y. Chu, "High Aspect Ratio In₂O₃ Nanowires: Synthesis, Mechanism and NO₂ Gas-Sensing Properties", *Sens. Actuators B*, **130**, 802–808 (2008).
- [11] A. Vomiero, M. Ferroni, E. Comini, G. Faglia, and G. Sberveglieri, "Insight into the Formation Mechanism of One-Dimensional Indium Oxide Wires", *Cryst. Growth & Design*, **10**, 140–145 (2010).
- [12] A. Walsh, J. L. F. Silva, S. H. Wei, C. Korber, A. Klein, L. F. J. Piper, A. DeMasi, K. E. Smith, G. Panaccione, P. Torelli, D. J. Payne, A. Bourlange, and R. G. Egdell, "Nature of the Band Gap of In₂O₃ Revealed by First-Principles Calculations and X-Ray Spectroscopy", *Phys. Rev. Lett.*, **100**, 167402–167405 (2008).
- [13] Z. R. Xiao, X. F. Fan, L. X. Guan, C. H. A. Huan, J. L. Kuo, and L. Wang, "First-Principles Study of the Magnetization of Oxygen-Depleted In₂O₃(001) Surfaces", *J. Phys. Condens. Mater.*, **21**, 272202–272207 (2009).
- [14] M.F.Al-Zubaidi and W.N.Ibrahim, "Increasing the conductivity of Cadmium Telluride Films", *J.Eng.&Tech.* **27**, 2682-2691 (2009).
- [15] C. Li, D. Zhang, S. Han, X. Liu, T. Tang, and C. Zhou, "Diameter Controlled Growth of Single-Crystalline In₂O₃ Nanowires and Their Electronic Properties", *Adv. Mater.*, **15**, 143–146 (2003).
- [16] T. Gao and T. Wang, "Catalytic Growth of In₂O₃ Nanobelts by Vapor Transport", *J. Cryst. Growth*, **290**, 660–664 (2006).
- [17] Chien-Ping Lee, H. Frank Chau, Wenlong Ma, and Nanlei Larry Wang, "The Safe Operating Area of GaAs-Based Heterojunction Bipolar Transistors", *IEEE Trans. on Electron Devices*, **53**, 11 (2006).
- [18] G.M.Zhen and X.D.Shey, "Thickness Dependence of Resistivity and optical Reflectance of ITO films", *Chinese Phys. Lett.*, **25**, 1380-1385 (2008).
- [19] U.P.Khairnar, D.S. Bhavsar, R.U.Vaidya, G.P. Bhavsar, "Optical Properties of thermally evaporated Cadmium telluride thin films", *J. Materials Chemistry and Physics*, **80**, 421-437 (2003).
- [20] C. Luis, B. Jimenez, A. Henery, P. Mendez, and A. Peynor, "Production and Characterization of Indium Oxide and Indium Nitride", *Brazilian J. of Physics* **36**(3B), 1017-1020 (2006).
- [21] Ch. Jung, Huang, K. Chien L, and S. Yan, "Structure Properties of Titanium Dioxide Thin Films in sintered temperature by the Sol-Gel Method", *Engineering Materials* **368**, 1465-1467 (2008).
- [22] S. Latitha, R. Sathyamoorthy, A. Subbarayan, "Modelling and Simulation Single Layer Anti-Reflective Coating", *J. Solar Energy materials and Solar cells* **90**, 694-703 (2006).
- [23] A.V.Vorontsov, E.N. Savinov, J. Zhengsheng, "Fabrication of Porous TiO₂ thin films prepared with low temperature for Photocatalytic degradation of Methylene Blue Solution", *J. Photochem. Photobiol. A: Chem.* **125**, 113-117 (1999).
- [24] S. Ryu and K. Takashi, "Preparation of Ge-GaAs Heterojunctions by vacuum Evaporation", *Jpn. J. Appl. Phys.* **4**, 850-853 (1965).
- [25] F.C. Jain and M.A. Melehy, "Grating add-drop filter Application resonator coupling", *Applied Physics letters* **27**, 36-38 (1975)
- [26] B.G. Streetman "Solid State Electronic Devices", prentice-Hall, Inc, printed Englewood, USA **126**, 12-24 (1980).
- [27] M. Yoshimoto, T. Nakanano, T. Yamashita and K. Suzuki, "MBE growth of InN on Si toward hot Barrier Structure in Si Devices", *IPAP Conf. Series* **1**, 186-189 (2000).
- [28] A.M. Green "Solar cells", translated by Y.M. Hassan, Univ. of Mosul, (1989).
- [29] J. Poortmans and V. Arkhipov, "Thin Films Solar Cells Fabrication Characterization And application", John Wiley and Sons (2007).
- [30] S. Goto and Y. Nomura, "Surface Cleaning of Si-Doped/Undoped GaAs Substrates", *Jpn. J. Appl. Phys.* **34**, 1180-1183 (1995).
- [31] A.G. Milnes and D.L. Feucht, "Heterojunction and Metal-Semiconductors Junctions", New York and London, (1972).